Cell Motility and the Cytoskeleton 49:189–199 (2001)

Regulation of Monomeric Dynein Activity by ATP and ADP Concentrations

Katsuyuki Shiroguchi and Yoko Y. Toyoshima*

Department of Life Sciences, Graduate School of Arts and Sciences, The University of Tokyo, Tokyo, Japan

Axonemal dyneins are force-generating ATPases that produce ciliary and flagellar movement. A dynein has large heavy chain(s) in which there are multiple (4–6) ATP-binding consensus sequences (P-loops) as well as intermediate and light chains, constituting a very large complex. We purified a monomeric form of dynein (dynein-*a*) that has at least three light chains from 14S dyneins of *Tetrahymena thermophila* and characterized it. In in vitro motility assays, dynein-*a* rotated microtubules around their longitudinal axis as well as translocated them with their plus-ends leading. ATPase activity at 1 mM ATP was doubled in the presence of a low level of ADP ($\geq$ 20 μM). Both ATPase activity and translocational velocities in the presence of ADP ($\geq$ 20 μM) fit the Michaelis-Menten equation well. However, in the absence of ADP ($<$ 0.1 μM), neither of the activities followed the Michaelis-Menten-type kinetics, probably due to the effect of two ATP-binding sites. Our results also indicate that dynein-*a* has an ATP-binding site that is very sensitive to ADP and affects ATP hydrolysis at the catalytic site. This study shows that a monomeric form of a dynein molecule regulates its activity by direct binding of ATP and ADP to itself, and thus the dynein molecule has an intramolecular regulating system. Cell Motil. Cytoskeleton 49:189–199, 2001.

Key words: motor; inner-arm; ATPase; cilia; *Tetrahymena*; ATP-binding site

INTRODUCTION

Dyneins and microtubules constitute an important motile system in eukaryotic cells. Dyneins utilize the energy derived from the hydrolysis of ATP to move cilia and flagella or to transport organelles and vesicles in the cytoplasm. All dyneins known so far move towards the minus end of microtubules. The motor domain of dynein is as large as 300 kDa and about ten times larger than that of kinesin [Koonce and Samsó, 1996]. Recent work on dynein genes has revealed that dynein motor domains have coserved multiple ATP-binding consensus sequences (P-loops) [Gibbons et al., 1991; Ogawa, 1991; Myster et al., 1999]. Dyneins are classified into three groups: cytoplasmic dyneins, axonemal outer-arm dyneins, and inner-arm dyneins [Gibbons, 1995].

Axonemal dyneins have many isoforms; there are monomers, dimers, and trimers, and 14 dynein genes have been identified in *Tetrahymena* [Xu et al., 1999; Asai, 2000]. The motile properties of several axonemal dyneins have been investigated in vitro, and it has been demonstrated that dyneins have remarkable versatility: rotational movement along the longitudinal axis of a microtubule [Vale and Toyoshima, 1988], oscillatory movement on a microtubule [Shingyoji et al., 1998], processive movement by a monomeric form of dynein [Sakakibara et al., 1999], and variation of processivity by ATP concentrations [Hirakawa et al., 2000]. These properties might be related to the diversity of the dynein molecules and/or the large size of the dynein complex, which includes heavy chain(s) and intermediate and light chains.

Contract grant sponsor: Grant-in-Aid for Scientific Research on Priority Areas (A) and a Grant-in-Aid for Scientific Research (B) from the Ministry of Education, Science, Sports and Culture.

*Correspondence to: Yoko Y. Toyoshima, 3-8-1 Komaba, Meguro-ku, Tokyo 153-8902, Japan. E-mail: cyytoyo@mail.ecc.u-tokyo.ac.jp

Received 29 March 2001; Accepted 11 May 2001

The versatility of dynein might be partly attributed to the multiple ATP-binding sites in a heavy chain and also other ATP-binding site(s) in the intermediate and light chain(s). The most N-terminal ATP-binding site of the motor domain of a heavy chain is thought to be the ATP hydrolytic site. However, the role of multiple ATP-binding sites remains to be elucidated, although it has been reported that multiple (up to 4) ATP molecules can bind to a monomeric form of sea urchin β dynein [Mocz and Gibbons, 1996; Mocz et al., 1998]. In addition, it has been reported that there are light intermediate chains with unknown roles that have an ATP-binding site [Gill et al., 1994; Hughes et al., 1995].

On the other hand, the axonemal disintegration of *Tetrahymena* and the flagellar beating of *Chlamydomonas* are inhibited by higher ATP concentrations, and ADP releases this inhibition [Kinoshita et al., 1995; Omoto et al., 1996]. However, it is not clear whether the activity of the dynein molecule is directly regulated by ATP and ADP or there is another regulating system in cilia and flagella that is sensitive to ATP and ADP.

To study the regulation of the dynein molecule by ATP and ADP, it is advantageous to use a monomeric form of the dynein molecule as material to avoid the complexity derived from multiple heads. Such a study may elucidate the role of multiple ATP-binding sites. Here, we purified a monomeric dynein (dynein-*a*) from the 14S dyneins of *Tetrahymena* cilia. A medium-scale preparation yielded enough dynein-*a* to perform biochemical assays. We investigated the ATPase activity and motility of dynein-*a* at various ATP and ADP concentrations and found that neither activity could be explained by simple Michaelis-Menten-type kinetics in a physiological condition. We suggest that dynein-*a* has a high-affinity ADP-binding site and at least two functional ATP-binding sites, one of which could be the high-affinity ADP-binding site.

MATERIALS AND METHODS

Preparation of 22S Dynein and 14S Dyneins

Dyneins were prepared from *Tetrahymena thermophila* (strain B-255) cilia as described [Toyoshima, 1987]. The cilia were isolated from the cell bodies with 8 mM dibucaine followed by demembranation with 0.5%(v/v) Nonidet- P40 in a dynein preparation buffer (DP-Buffer; 10 mM Hepes-NaOH, pH 7.4, 4 mM $MgCl_2$, 100 mM NaCl, 1 mM EGTA) with 0.1 mM PMSF. The crude dynein was extracted from the axonemes with a DP-Buffer containing 0.6 M NaCl and 0.1 mM PMSF for 30 min on ice and centrifuged at 25,000*g* for 10 min. The extract was applied onto 30 ml of a 5–20% (w/v) sucrose density gradient in a DP-Buffer with 0.1 mM PMSF and 0.1 mM ATP and centrifuged with a Hitachi RPS 27-3 rotor at 26,000 rpm for 16 h at 2°C. Fractions of 1.5 ml were collected from the bottom of the gradient. Fractions 1–5 and 10–13 of 23 fractions usually corresponded to 22S and 14S dyneins, respectively.

Subfractionation of 14S Dyneins

Fourteen S dyneins were subfractionated using a high-performance liquid chromatography system (Tosoh Co.) with a MonoQ 5/5 column (Pharmacia). Fractions of 14S dyneins from the sucrose density-gradient centrifugation were diluted twice to reduce the final NaCl concentration to 50 mM and loaded on the column at a flow rate of 0.5 ml/min. Proteins were eluted with a linear 0–0.4 M NaCl gradient in a DP-Buffer containing 10% (w/v) sucrose. Each fraction of 0.5 ml was collected and stored in liquid N_2 after addition of 1 mM DTT. Further experiments were usually performed within a week, although dyneins maintained their motile activity for 1 month when stored in liquid N_2.

Preparation of Tubulin, Microtubules, and Polarity-Marked Microtubules

Tubulin was prepared from porcine brain and purified by phosphocellulose chromatography [Sloboda and Rosenbaum, 1982].

Microtubules were polymerized from the purified tubulin in an assembly buffer (80 mM Pipes-NaOH, pH 6.8, 1 mM $MgCl_2$, 1 mM EGTA) with 1 mM GTP and 10% (v/v) DMSO for 30 min at 37°C. The polymerized microtubules were stabilized by the addition of 20 μM paclitaxel (Wako Pure Chemical Industries, Ltd.).

Polarity-marked microtubules were prepared as previously described [Vale and Toyoshima, 1988]. The salt-extracted axonemes (~3 mg/ml) were sonicated for 3 min and incubated with N-ethylmaleimide-modified tubulin (0.15 mg/ml) and unmodified tubulin (1.5 mg/ml) in an assembly buffer in the presence of 3 mM GTP, 10% (v/v) DMSO, and 2 mM DTT for 30 min at 37°C. The polymerization was terminated by addition of a twofold volume of an assembly buffer with 10% (v/v) DMSO and 40 μM paclitaxel.

Sedimentation Analysis

To examine the sedimentation profile of dynein-*a*, the purified dynein-*a* (0.5 ml of 100 μg/ml) was analyzed by centrifugation in 15–30% (w/v) sucrose density gradients (33,000 rpm, 19 h, 2°C) with an RPS 50-2 rotor (Hitachi). The chymotryptic fragments of 22S dynein were used as markers for single- and double-headed dynein molecules [Toyoshima, 1987].

Electron Microscopy

One drop of a freshly prepared specimen containing 10 ng/ml of dynein-*a* was applied to a carbon film

and stained with 1% uranyl acetate. Samples were observed with a H-7500 electron microscope (Hitachi) with a magnification of ×50,000 operating at 100 kV.

ATPase Assay

The ATPase assay was performed using Enzcheck (Molecular Probes) in an Assay buffer (10 mM Pipes-KOH, pH 7.0, 50 mM K-acetate, 4 mM $MgSO_4$, 1 mM EGTA, 1 mM DTT) at 5–1,000 μM ATP and 10–1,000 μM ADP at 25°C by monitoring the absorbance at 360 nm. To keep ATP concentrations constant and ADP concentrations low, 2 mM creatine phosphate and 0.5 mg/ml creatine kinase were added. The ADP level was estimated by the equilibrium constant of creatine kinase ($K = 1.6 \times 10^2$). We made sure that this equilibrium constant was appropriate in the Assay buffer by determining the ADP concentration at a detectable range.

In Vitro Motility Assay

Dynein-*a* (50 μg/ml) was applied to a flow chamber and adsorbed onto the glass for 2 min. To remove the unadsorbed dyneins and block the surface of the glass, 3 vol (1 vol ~15 μl) of 0.5 mg/ml BSA in an Assay buffer was perfused into the chamber. After a 2-min incubation, the excess BSA was washed away with 3 vol of the Assay buffer. Then, 3 vol of paclitaxel-stabilized microtubules or polarity-marked microtubules (30 μg/ml) was applied for 2 min and washed with 3 vol of the Assay buffer. Finally, 10–2,000 μM ATP (and 20 μM ADP) with 10 μM paclitaxel in the Assay buffer (3 vol) was perfused, and the movements of microtubules were observed by dark-field illumination with an objective of ×40 and recorded with a VTR. The assay was performed at 25 ± 1°C. To keep ATP concentrations constant and ADP concentrations low, 2 mM phosphoenolpyruvate and 0.1 mg/ml pyruvate kinase were added. ADP concentration was estimated by the equilibrium constant of pyruvate kinase ($K = 2.0 \times 10^5$). Creatine phosphate and creatine kinase, which were used in the ATPase assay, were not used in the motility assays because creatine kinase (> 0.5 mg/ml) inhibited the translocation of microtubules.

The velocities of microtubules that translocated continuously for at least 10 μm were analyzed using the Measure program [Sheetz et al., 1986]. The rotational frequency was measured from the record of polarity-marked microtubules that rotated continuously at least 7 times.

UV Cleavage, Polyacrylamide Gel Electrophoresis, and Protein Determination

UV cleavage was performed as described [Gibbons et al., 1987]. Dynein-*a* was incubated for 30 min on ice with 50 μM ATP and 50 μM vanadate (Sigma, St. Louis, MO) in the DP-Buffer, irradiated by V at 365 nm (UVL-28, UVP) mounted about 5 mm above the samples.

SDS-polyacrylamide gel electrophoresis (PAGE) was performed on 10% (w/v), 6% (w/v), and 4% (w/v) slab gels [Laemmli, 1970]. SDS-urea-PAGE was carried out as described [Toyoshima, 1987]. Gels were stained with Coomassie Brilliant Blue R-250.

Protein concentration was determined by the method of Read and Northcote [1981] using BSA as a standard.

RESULTS

Subfractionation of 14S Dyneins and Dynein-*a*

Fourteen S dyneins were subfractionated with a MonoQ column (Fig. 1A). There seemed to be at least six dynein subspecies in the fractions eluted with a NaCl gradient (Fig. 1B), and no dynein heavy chains were detected in the flow-through and after 0.4 M NaCl elution. Each of the fractions containing dynein heavy chains (*a–f*) was able to move microtubules in the motility assay. The last peak after peak-*f* was not a dynein, judging from the absence of heavy chains.

We focused on the dynein in peak-*a* (dynein-*a*) and characterized it, since it was clearly separated from the others and showed a single band in the heavy-chain region on both the SDS-gel (Fig. 1B) and SDS-urea gel electrophoresis (data not shown). Proteins of 43, 35, and 30 kDa were identified as light-chain components of the dynein-*a* complex because they co-sedimented with the dynein-*a* heavy chain in the subsequent sucrose density-gradient centrifugation (Fig. 2A,B). No associated proteins between 14 and 30 kDa were detected in SDS 15% polyacrylamide gels (data not shown).

Direction of the Movement and the Rotational Activity of Dynein-*a*

We examined the direction of the movement and the rotational activity of dynein-*a* in the motility assay in the absence of phosphoenolpyruvate and pyruvate kinase. Polarity-marked microtubules were translocated with their plus-ends leading and rotated around the longitudinal axis. Therefore, dynein-*a* moved the microtubules to the minus-end direction. The mean pitch of the rotation was 250 ± 70 nm (mean ± s.d., n = 31) in the velocity range of 0.1–3.0 μm/s. The direction of microtubule rotation was always clockwise when viewed from the minus-end of the microtubules, which was determined by focusing the objective slightly above the glass surface and observing the curved ends of the polarity-marked microtubules as they came into and out of focus during rotation. The rotation was occasionally blocked when the curved end was physically hindered by the glass surface. Even when the rotation was blocked,

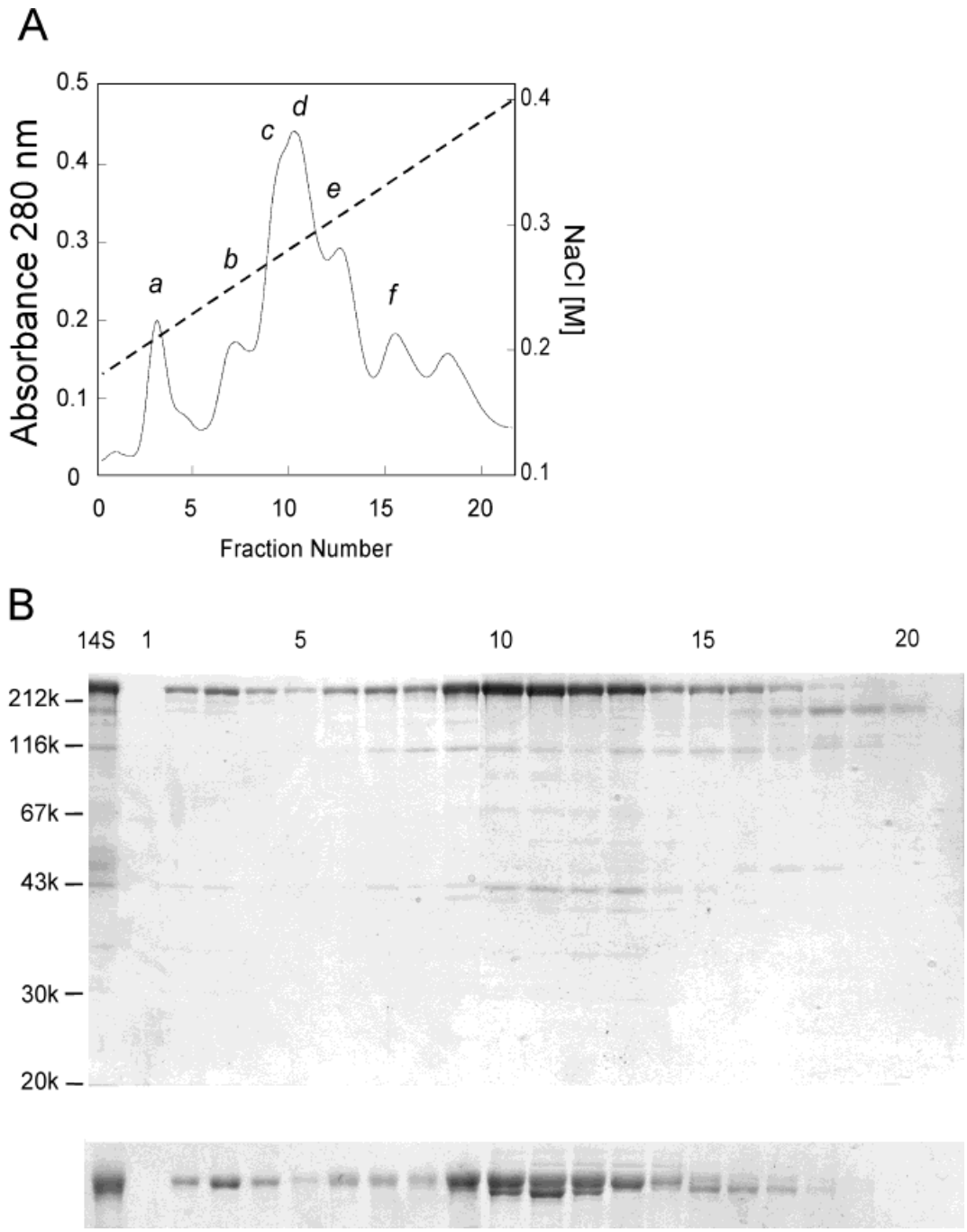

Fig. 1. Fractionation of the 14S dyneins by anion-exchange chromatography on a MonoQ column. **A:** Solid line, absorbance at 280 nm. Dashed line, NaCl concentration in an elution buffer. *a–f*: peak fractions that contain dynein heavy chains. **B: Top:** SDS-PAGE of 14S dyneins and the fractions in A in a 10% gel. **Bottom:** High-molecular-weight region in a 4% gel of SDS-PAGE of the same fractions as in the top panel, showing different species of dynein heavy chains. Left-hand numbers: molecular weight markers.

the translocation persisted, resulting in the curved end of the polarity-marked microtubules on the glass pointing to the right of the axis as viewed from the minus end. This observation is consistent with the clockwise rotation produced by dynein-*a*.

Morphology of Dynein-*a*

It is important to understand the morphology of dynein-*a*. To determine the number of head(s) of dynein-*a*, we carried out sedimentation analysis, UV cleavage, and electron microscopy.

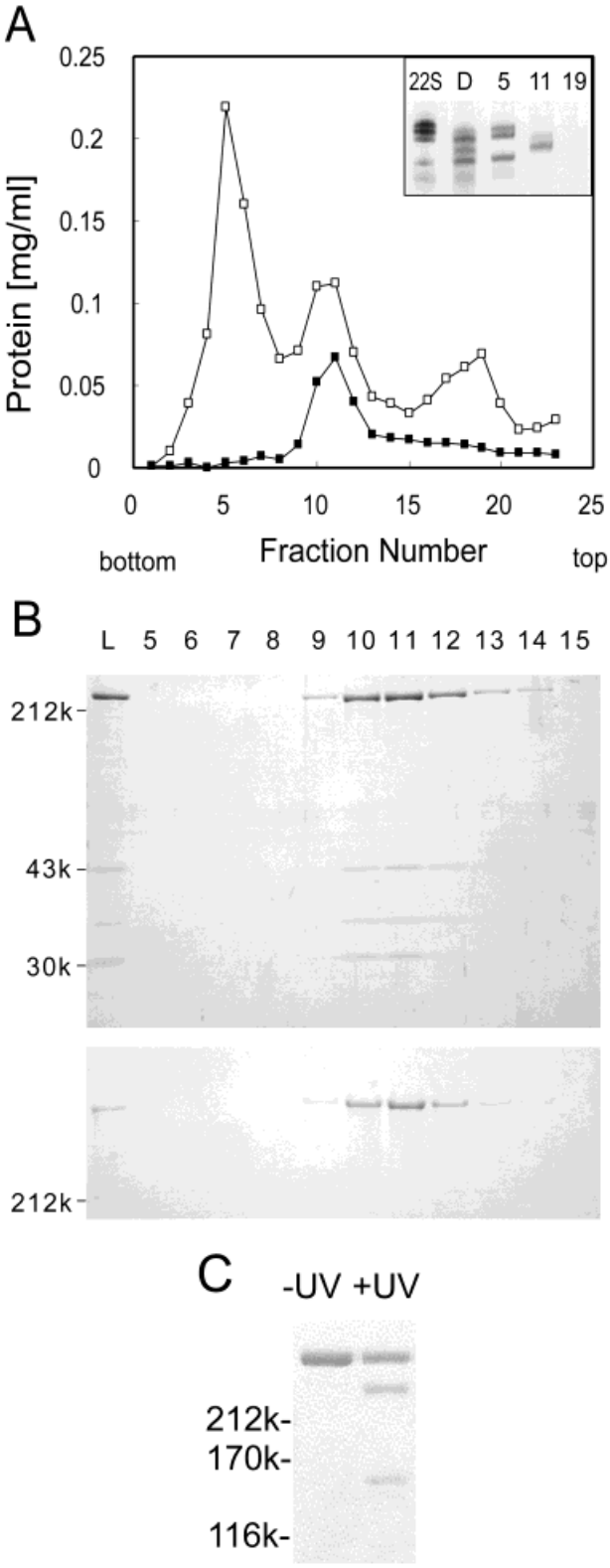

Dynein-*a* was sedimented on the sucrose density gradients simultaneously with the single- and double-headed dynein fragments that were produced from chymotryptic digention of 22S dynein [Toyoshima, 1987]. The peak of dynein-*a* (fraction11 in Fig. 2A,B) was in the same position as the peak of chymotryptic fragments of 22S dynein, which is a monomeric or single-headed form.

The Heavy chain of dynein-*a* was cleaved into two polypeptides by UV irradiation in the presence of ATP and vanadate (Fig. 2C). This shows that dynein-*a* has a common feature of dyneins already discovered [Kagami and Kamiya, 1992; Muto et al., 1994]. This result indicates that dynein-*a* is composed of a single heavy chain.

In the electron micrographs of a negatively stained specimen, globular particles were scattered throughout the field (Fig. 3A,B). The diameter of the globular particle was about 13 nm, and a cavity was observed in some particles. These features have been seen in the globular domains of other dyneins [Toyoshima, 1987; Samsó et al., 1998; Sakakibara et al., 1999].

From these observations and the SDS gel analysis, we concluded that dynein-*a* is a single-headed molecule comprise of a single heavy chain. To analyze the role of multiple ATP-binding sites of a dynein molecule, it is important to study a dynein that is single-headed and is comprised of a single heavy chain. Dynein-*a* is a good candidate for this purpose. Therefore, we investigated the ATPase activity and motile properties of dynein-*a* in more detail.

ATPase Activity of Dynein-*a*

We measured the ATPase activity of dynein-*a* at various concentrations of ATP and ADP. During the course of these experiments, we noticed that the ATPase activity of dynein-*a* was dependent on the ADP concentration of the assay solution. Therefore, we first measured

Fig. 2. Sucrose density-gradient centrifugation analysis of dynein-*a* purified with a MonoQ column and the UV cleavage experiment. **A:** *Solid squares*, protein concentration of dynein-*a*. *Open squares*, protein concentration of markers; single- and double-headed dyneins derived from 22S dynein by α-chymotryptic digestion. **Inset:** 3.2% SDS-urea-PAGE of 22S dynein. 22S dynein digested (D), and three peak fractions (indicated as fraction numbers). Bands of fractions 5 and 11 indicate two- and one-headed dyneins, respectively, which were shown by Toyoshima [1987]. There was no dynein heavy chain in fraction 19. **B: Top:** SDS-PAGE of dynein-*a* and the fractions in A in a 10% gel. **Bottom:** High-molecular-weight region in a 4% gel of SDS-PAGE of same fractions as in the top panel, showing a single heavy chain. L, dynein-*a* loaded. Top numbers, fraction numbers. Left-hand numbers, molecular weight markers. **C:** 6% gel of SDS-PAGE of dynein-*a* cleaved by UV irradiation for 30 min on ice in the presence of 50 μM ATP and 20 μM vanadate. Left-hand numbers, molecular weight markers.

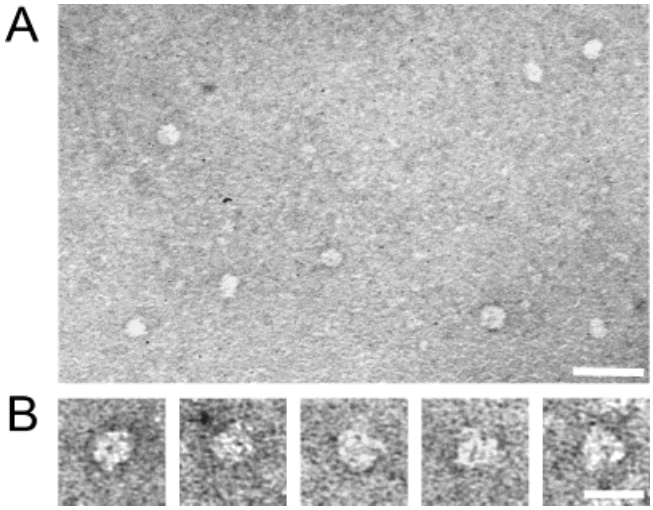

Fig. 3. Electron micrographs of dynein-*a* negatively stained with 1% uranylacetate. **A:** General view of dynein-*a*. Bar = 50 nm. **B:** Selected images at higher magnification. Bar = 20 nm.

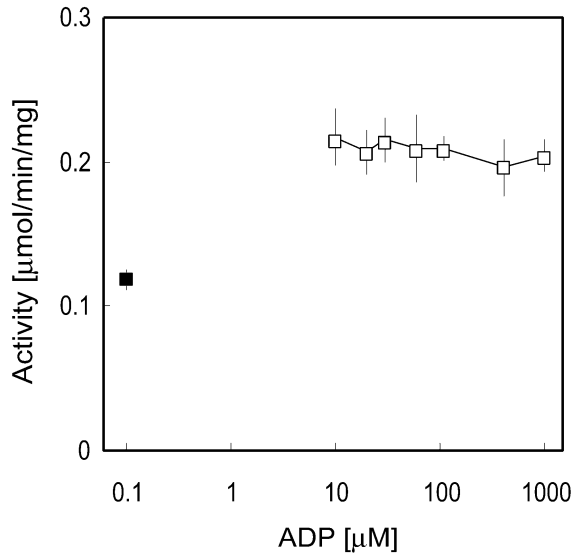

Fig. 4. ATPase activity of dynein-*a* at 1 mM ATP and various ADP concentrations. *Open squares*, activities in the presence of ADP (10–1,000 μM). **Solid square**, activity in the presence of creatine phosphate and creatine kinase to keep ADP concentration low (~0.1 μM). Error bars = s.d.

the activity at 1 mM ATP by changing ADP concentrations (Fig. 4). The activity was almost constant in the ADP concentration range from 10 μM to 1 mM at the beginning of each assay. ADP concentration contaminated from ATP was determined spectrophotometrically by monitoring absorbance of NADH in the enzyme coupling system. Next, we tried to keep the ADP concentration low by using creatine phosphate and creatine kinase to consume ADP produced by catalysis. Creatine phosphate and creatine kinase themselves did not affect the ATPase activity of dynein-*a* (within 100 ± 5% of the activity in the absence of creatine phosphate and creatine kinase at 1 mM ATP). At 1 mM ATP, the activity in the presence of 10 μM ADP (0.22 ± 0.02 (mol/min/mg; mean ± s.d.) was twice the activity in the absence (<0.1 μM) of ADP (0.11 ± 0.01 μmol/min/mg; mean ± s.d.) (Fig. 4). Since controlling ADP concentrations below 10 μM in the assay was difficult, we next measured the activity depending on ATP concentrations (5–1,000 μM) with the ADP concentration fixed at <0.1, 20, 1,000 μM (Fig. 5A). Eadie-Hofstee plots (Fig. 5B) show that, in the presence of 20 and 1,000 μM ADP, the activity fit well with the Michaelis-Menten equation (K_m = 9.1 ± 0.4 μM, k_{cat} = 0.20 ± 0.00 μmol/min/mg at 20 μM ADP, K_m = 44 ± 3 μM, k_{cat} = 0.22 ± 0.01 μmol/min/mg at 1 mM ADP; mean ± s.e.). The larger value for the K_m in the presence of 1 mM ADP than in the presence of 20 μM ADP seems to be due to the competitive inhibition of ATP by ADP. In the absence of ADP (< 0.1 μM), on the other hand, the activity did not fit a linear relationship in the Eadie-Hofstee plots, indicating that the activity did not follow simple Michaelis-Menten-type kinetics.

Velocity of Microtubule Translocation Driven by Dynein-*a*

We measured the velocity of microtubule translocation induced by dynein-*a* in in vitro motility assays at various ATP concentrations in the presence of ADP (20 μM at the beginning of each assay) and the absence of ADP (< 0.1 nM, in the presence of phosphoenolpyruvate and pyruvate kinase) (Fig. 6A). Phosphoenolpyruvate and pyruvate kinase did not alter the velocity of microtubules (within 100 ± 1% of the mean velocity in the absence of phosphoenolpyruvate and pyruvate kinase at 1 mM ATP). When less than 30 μg/ml dynein-*a* was used in the assay, the microtubules moved unstably, sometimes stopped and stayed immobile for a while, and then started to move again. Thus, 50 μg/ml dynein-*a* was applied to the assay chamber, since microtubules moved stably and smoothly at that concentration of dynein-*a*. It was difficult to determine the velocities of microtubules at less than 50 μM ATP in the absence of phosphoenolpyruvate and pyruvate kinase, that can keep ATP concentration constant, since the velocities were reduced soon after applying ATP due to the hydrolysis by dynein. At 2 μM ATP, the translocation of microtubules by dynein-*a* was hardly observed, whereas in the presence of phosphoenolpyruvate and pyruvate kinase, dynein-*a* stably moved the microtubules.

Figure 6B shows the velocities of microtubules in Eadie-Hofstee plots. In the range of 100–1,000 μM ATP, the velocities of microtubules in the presence of 20 μM ADP were almost the same as those in the absence of ADP.

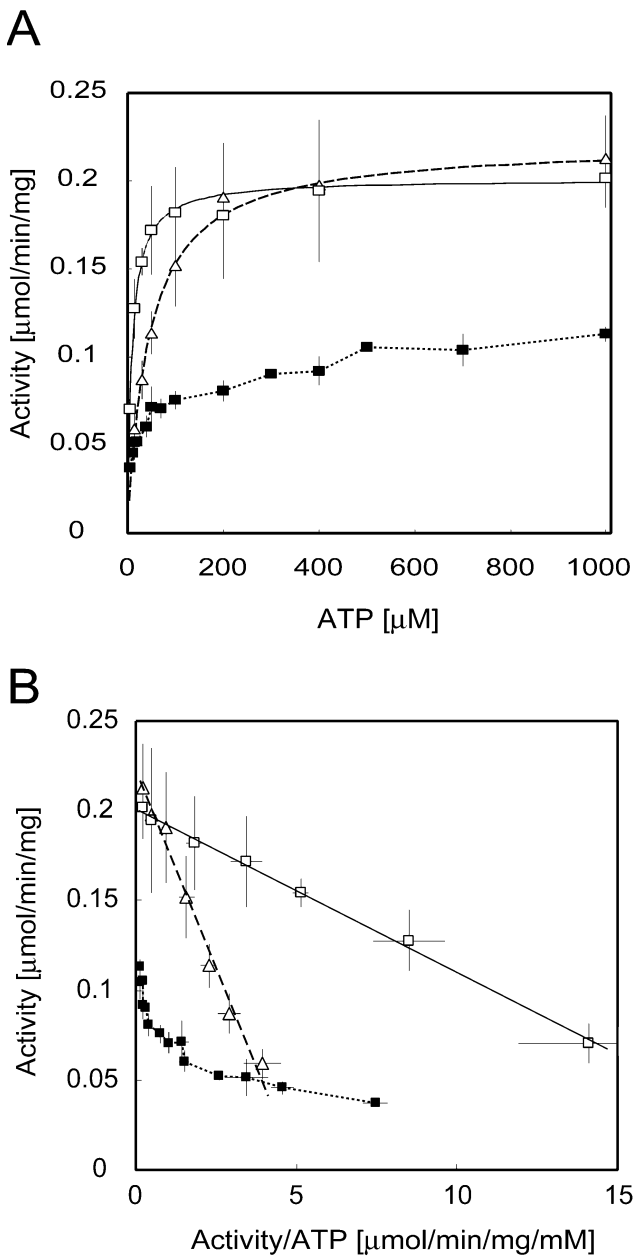

Fig. 5. ATPase activity of dynein-*a* at various ATP concentrations. **A:** *Open squares* and *open triangles*, activities in the presence of 20 μM ADP and 1 mM ADP, respectively, each fitted by the Michaelis-Menten equation (K_m = 9.1 ± 0.4 μM, k_{cat} = 0.20 ± 0.00 μmol/min/mg at 20 μM ADP presented by a solid line, K_m = 44 ± 3 μM, k_{cat} = 0.22 ± 0.01 μmol/min/mg at 1 mM ADP presented by a broken line; mean ± s.e.). *Solid squares*, activities in the presence of creatine phosphate and creatine kinase to keep ADP concentration low (<0.1 μM), linked by a dotted line. **B:** Eadie-Hofstee plots. Symbols are the same as in A. The plots in the presence of 20 μM ADP and 1 mM ADP fit to a straight line. Each plot in the absence of ADP (<0.1 μM) is linked by a dotted line in the order of ATP concentrations. Error bars = s.d.

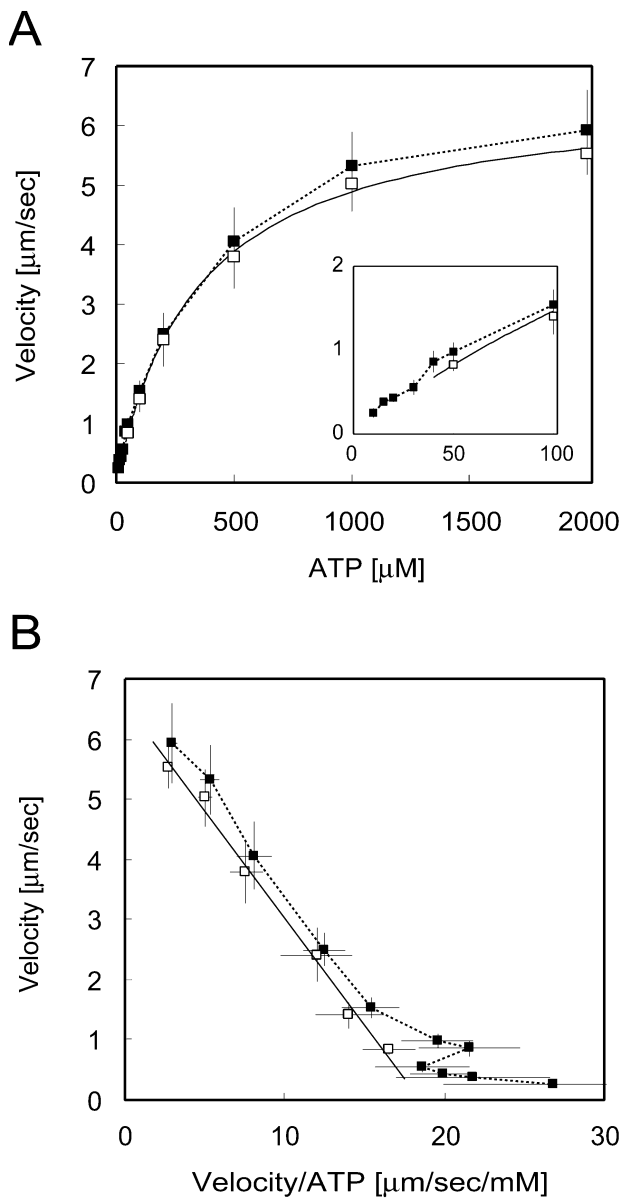

Fig. 6. Gliding velocity of microtubules. **A:** *Open squares*, velocities in the presence of 20 μM ADP fitted by the Michaelis-Menten equation (K_m = 350 ± 10 μM, V_{max} = 6.6 ± 0.1 μm/sec presented by a solid line; mean ± s.e.). *Solid squares*, velocities in the presence of phosphoenolpyruvate and pyruvate kinase to keep ADP concentration low (<0.1 nM) linked by a dotted line. **Inset:** Magnification in the range of low ATP concentrations. **B:** Eadie-Hofstee plots. Symbols are the same as in A. The plots in the presence of 20 μM ADP fit to a straight line. Each plot in the absence of ADP (<0.1 nM) is linked by a dotted line in the order of ATP concentrations. Error bars = s.d.

Similarly to the ATPase assay, in the presence of ADP (20 μM), the velocity of microtubules fitted Michaelis-Menten kinetics (K_m = 350 ± 10 μM, V_{max} = 6.6 ± 0.1 μm/sec; mean ± s.e.) well. In the absence of ADP (< 0.1 nM), the curve was not linear in the range of less than 100 μM ATP and was thus not explained by a single K_m and V_{max}.

DISCUSSION

Subspecies of 14S Dyneins and Dynein-*a*

We subfractionated 14S dyneins by anion exchange column chromatography. The profile of the protein separation was similar to the results reported by Muto et al [1994]. They described that their peak-*c* contained two separate dynein subspecies. Their peak-*c* was resolved to two peaks in our preparation, *c*, *d*, each of which seemed to have a single heavy chain (Fig. 1B). Accordingly, our peak-*e* and -*f* corresponded to their peak-*d* and -*e*.

It has been reported that there are at least nine heavy-chain genes encoding inner-arm dyneins in *Tetrahymena* [Xu et al., 1999; Asai, 2000]. Our results showed that the 14S dyneins of *Tetrahymena* contain at least six heavy chains (Fig. 1A,B). The heavy chain of peak-*b* sometimes separated into two bands, which might indicate the existence of seven heavy chains in 14S dyneins. These possible seven heavy chains of 14S dyneins and two heavy chains sedimented together at 18 S [Mobberley et al., 1999] could explain the nine heavy-chain genes already discovered. The complexity of the inner-arm dyneins in *Tetrahymena* appears to be similar to that of *Chlamydomonas*, which is reported to have eight heavy chains [Kagami and Kamiya, 1992].

Although inner-arm dyneins have been shown to have essential and complex properties in ciliary movement, they have not been well studied from a biochemical point of view because it has been difficult to purify them in large amounts. Here, we report the purification of inner-arm dynein-*a* from *Tetrahymena* cilia in sufficient quantities for biochemical assays.

It was shown that dynein-*a* is a monomeric form of single heavy chain by SDS-electrophoresis (Figs. 1B, 2B), SDS-urea gel electrophoresis (data not shown), sucrose density-gradient centrifugation (Fig. 2A,B), UV cleavage (Fig. 2C), and electron microscopy (Fig. 3A,B). Our preliminary experiments showed that dynein-*f* sedimented at the same position in sucrose density gradients as dynein-*a* and was cleaved into two polypeptides by UV irradiation, which suggests that dynein-*f* is also monomeric and single-headed. There may be more species of monomeric dyneins in the 14S dyneins of *Tetrahymena*, as in *Chlamydomonas*, in which there seem to be six monomeric dyneins in inner-arm dyneins [Kagami and Kamiya, 1992].

Dynein-*a* also has at least three light chains (Fig. 2B) and the 43-kDa protein is known to be actin [Muto et al., 1994], while the others have not been identified yet. In *Chlamydomonas*, some dyneins have a Ca^{2+}-binding protein as a light chain [Piperno et al., 1992; King and Patel-King, 1995] and it has been reported that some light chains regulate dynein activity by phosphorylation [Hamasaki et al., 1995; Inaba et al., 1998]. Further analysis of the light chains of dynein-*a* promises to reveal more about the functions and regulation of dynein activity.

Rotational Activity of Dynein-*a*

Dynein-*a* produced a rotational translocation of microtubules. The mixture of 14S dyneins from *Tetrahymena* and at least 5 subspecies of *Chlamydomonas* inner-arm dyneins has been found to rotate microtubules around the longitudinal axis [Vale and Toyoshima, 1988; Kagami and Kamiya, 1992]. In addition, our preliminary observations indicated that dyneins in peak-*c*, -*d*, and -*e* (Fig. 1A) also have this property, suggesting that many or all of the inner-arm dyneins from *Tetrahymena* and *Chlamydomonas* are able to rotate microtubules.

Translocation and rotation induced by dynein-*a* were not coupled tightly, since dynein-*a* moved the microtubules forward even when the curved end of the polarity-marked microtubules blocked the rotation. This feature is similar to 14S dyneins and Ncd, a kinesin-like protein. The pitch of dynein-*a* rotation ($\sim$250 nm) is almost half that of 14S dyneins ($\sim$540 nm) and is similar to those of inner-arm dyneins from *Chlamydomonas* (200–600 nm) and Ncd ($\sim$300 nm). These do not fit microtubule lattices of 3-, 5-, 8-, and 13-start helices and are different from kinesin, which moves along the 13-start helix [Ray et al., 1993]. This study indicated that even a monomeric dynein caused the rotation as well as the translocation of microtubules. It will be interesting to analyze the mechanism of the rotation of monomeric dynein at the single-molecular level.

Activities of Dynein-*a* Depending on ATP and ADP Concentrations

Our results showed that the ATPase and motile activities of dynein-*a* were significantly affected by ADP. ATPase activity in the presence of 20 μM ADP was almost twice the activity of dynein-*a* in the absence of ADP (< 0.1 μM) (Fig. 5A). Furthermore, ATPase and motile activity in the absence of ADP did not follow simple Michaelis-Menten kinetics, in which ATPase and motile activities depended on the presence of low concentrations of ADP (Figs. 5B, 6B). These results suggest that the activity of dynein-*a* is regulated by the binding of ADP to an ATP-binding site that has high affinity for ADP. Recently, it was reported that the inner-arm dynein-*a* of *Chlamydomonas* with ATP did not translocate microtubules in the absence of ADP but did so in the presence of ADP [Yagi, 2000]. This shows that ADP stimulates the motile activity of the inner-arm dynein. These properties as a result of a monomeric form of dynein-*a* indicate that a monomeric dynein molecule itself can change its activity by the binding of ATP and ADP. In cilia and flagella, the wave propagation might be

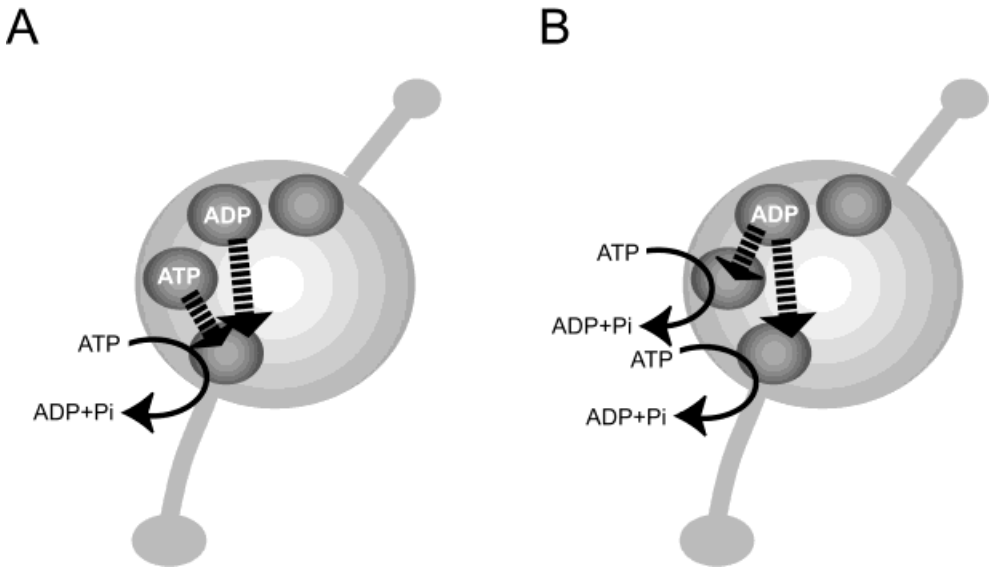

Fig. 7. Two possible mechanisms that regulate ATP hydrolytic activity of dynein-*a*. Four conserved nucleotide-binding sites (*small circles*) are in a motor domain (the *largest circle*) with a stalk (above) and a stem (below). *Solid arrows* indicate hydrolysis of ATP to ADP and Pi. *Dotted arrows* show the regulation of hydrolytic activity by the binding of nucleotide at a noncatalytic nucleotide-binding site. **A:** The hydrolytic activity is regulated by binding of ATP and ADP at noncatalytic site(s). ADP that binds to the third site in this figure may bind to the second site and regulate the activity. **B:** There are two hydrolytic sites that are regulated by binding of ADP at a noncatalytic site. Here, to explain simply, we locate the second and the third nucleotide-binding sites in a heavy chain; however, there is a possibility that these sites are in light chains.

attributed to the regulation of dynein activity by the binding of ATP and ADP.

To explain the data of ATPase activity in the absence of ADP, which seems to be a combination of two straight lines (Fig. 5B), we present two possibilities here, considering that two straight lines correspond to two states of dynein activity. The first possibility is that the catalytic site in a dynein molecule is single and this site has two states of activity which are switched by the binding of ATP and ADP to other noncatalytic ATP-binding site(s) (Fig. 7A). If the ATP concentration of the cross point of two straight lines in Figure 5B ($\sim$100 μM) corresponds to the dissociating constant of a noncatalytic ATP-binding site that causes the switching of two states, the previous report about a nucleotide dissociating constant (10^{-4}–10^{-5} M) of sea urchin β dynein supports this first possibility [Mocz and Gibbons, 1996]. The second possibility is that dynein-*a* has two ATP catalytic sites that have different affinity for ATP and work independently from each other, and that both are regulated by ADP binding to another ATP-binding site (Fig. 7B). It means that the two straight lines may represent two catalytic sites in a dynein molecule. For the outer-arm dynein, it has been reported that the ATPase activity of sea urchin β dynein decreases according to the extent of photocleavage at the V1 site of the dynein heavy chains that corresponds to P1, the most N-terminal P-loop of the four [Gibbons et al., 1987, 1991; Mocz et al., 1988]. Consequently, β dynein seems to have a single catalytic site. However, an inner-arm dynein may have more than a single catalytic ATP-binding site in a dynein molecule.

We first described the ATP-binding site that has high affinity for ADP. This site does not seem to be a P1 site. In the first possibility, although the ADP high-affinity site is presented as the third site (Fig. 7A), this site could be the same as the noncatalytic ATP binding site (the second site). On the other hand, for the second possibility, it might be the third site, which is different from the P1 and the second ATP catalytic sites (Fig. 7B). Of course there could be other more complex possibilities, however, at least two functional ATP-binding sites must exist in a dynein molecule to explain our data.

Actin, the 43-kDa light chain of dynein-*a*, has an ATP-binding site. On the other hand, it is unknown whether 35- and 30-kDa light chains have an ATP-binding site or not. One of the functional ATP-binding sites suggested here is thought to be a P1 site that hydrolyzes ATP, and another site(s) may also be in a heavy chain as a conserved ATP-binding site of dynein species. Alternatively, there is a possibility that another site(s) might be in a light chain [Hughes et al., 1995]. Here, to explain simply, we present the second and the third sites in a heavy chain in Figures 7A,B.

The motility data could not be explained by simple Michaelis-Menten kinetics in the absence of ADP (< 0.1 nM) either (Fig. 6B). The motile activity of dynein-*a*

should be related to the ATPase activity and might be explained by the same possibilities above. However, the explanation of the motility data may be more complex, since the velocities of microtubules may be affected by multiple dyneins interacting with a single microtubule.

The ATPase activity of dynein-*a* at 1 mM ATP was approximately doubled in the absence of ADP (Fig. 5A). However, the velocity of microtubules did not change as much (Fig. 6A). This may be due to the difference between activities in the presence and absence of microtubules. Alternatively, this might be because dynein-*a* has activities other than microtubule translocation that depend on ATP hydrolysis, or the efficiency of energy transduction by dynein-*a* changes according to the concentration of ADP.

The previous works to show that axonemal or flagellar motile activities are regulated by ATP and ADP could not distinguish that the regulation system exists within a dynein molecule or involves other axonemal components. Here we showed that both the ATPase and motile activities of a monomeric form of a dynein are regulated by direct binding of ATP and ADP to itself, and thus we can conclude that this regulating mechanism exists within a monomeric form of a dynein molecule. These results suggest the functional roles of multiple ATP-binding sites of a dynein at the molecular level. This study can be a significant first step toward elucidating the complete function and mechanism of multiple ATP-binding sites in a dynein molecule, which might explain the versatility of dynein motility. Future studies of a single-headed dynein, such as site-directed mutagenesis and modifications of P-loops together with motility analysis, will improve our understanding of dynein function.

ACKNOWLEDGMENTS

We thank Dr. M. Edamatsu for his advice on purification of dynein-*a*. We are also grateful to Dr. D. J. Asai for reading through the manuscript and comments.

REFERENCES

Asai DJ. 2000. The analysis of dynein structure and function in ciliated protozoa. Jpn J Protoz 33:15–27.

Gibbons IR. 1995. Dynein family of motor proteins: present status and future questions. Cell Motil Cytoskeleton 32:136–144.

Gibbons IR, Gibbons BH, Mocz G, Asai DJ. 1991. Multiple nucleotide-binding sites in the sequence of dynein β heavy chain. Nature 352:640–643.

Gibbons IR, Lee-Eiford A, Mocz G, Phillipson CA, Tang W-JY, Gibbons BH. 1987. Photosensitized cleavage of dynein heavy chains. Cleavage at the "V1 site" by irradiation at 365 nm in the presence of ATP and vanadate. J Biol Chem 262:2780–2786.

Gill SR, Cleveland DW, Schroer TA. 1994. Characterization of DLC-A and DLC-B, two families of cytoplasmic dynein light chain subunits. Mol Biol Cell 5:645–654.

Hamasaki T, Barkalow K, Satir P. 1995. Regulation of ciliary beat frequency by a dynein light chain. Cell Motil Cytoskeleton 32:121–124.

Hirakawa E, Higuchi H, Toyoshima YY. 2000. Processive movement of single 22S dynein molecules occurs only at low ATP concentrations. Proc Natl Acad Sci 97:2533–2537.

Hughes SM, Vaughan KT, Herskovits JS, Vallee RB. 1995. Molecular analysis of a cytoplasmic dynein light intermediate chain reveals homology to a family of ATPases. J Cell Sci 108:17–24.

Inaba K, Morisawa S, Morisawa M. 1998. Proteasomes regulate the motility of salmonid fish sperm through modulation of cAMP-dependent phosphorylation of an outer arm dynein light chain. J Cell Sci 111:1105–1115.

Kagami O, Kamiya R. 1992. Translocation and rotation of microtubules caused by multiple species of *Chlamydomonas* inner-arm dynein. J Cell Sci 103:653–664.

King SM, Patel-King RS. 1995. Identification of a Ca^{2+}-binding light chain within *Chlamydomonas* outer arm dynein. J Cell Sci 108:3757–3764.

Kinoshita S, Miki-Noumura T, Omoto CK. 1995. Regulatory role of nucleotides in axonemal function. Cell Motil Cytoskeleton 32:46–54.

Koonce MP, Samsó M. 1996. Overexpression of cytoplasmic dynein's globular head causes a collapse of the interphase microtubule network in *Dictyostelium*. Mol Biol Cell 7:935–948.

Laemmli UK. 1970. Cleavage of structural proteins during the assembly of the head of bacteriophage T4. Nature 227:680–685.

Mobberley PS, Sullivan JL, Angus SP, Kong X, Pennock DG. 1999. New axonemal dynein heavy chains from *Tetrahymena thermophila*. J Eukaryot Microbiol 46:147–154.

Mocz G, Gibbons IR. 1996. Phase partition analysis of nucleotide binding to axonemal dynein. Biochemistry 35:9204–9211.

Mocz G, Helms MK, Jameson DM, Gibbons IR. 1998. Probing the nucleotide binding sites of axonemal dynein with the fluorescent nucleotide analogue 2′(3′)-O-(-N-Methylanthraniloyl)-adenosine 5′-triphosphate. Biochemistry 37:9862–9869.

Mocz G, Tang W-JY, Gibbons IR. 1988. A map of photolytic and tryptic cleavage sites on the β heavy chain of dynein ATPase from sea urchin sperm flagella. J Cell Biol 106:1607–1614.

Muto E, Edamatsu M, Hirono M, Kamiya R. 1994. Immunological detection of actin in the 14S ciliary dynein of *Tetrahymena*. FEBS Lett 343:173–176.

Myster SH, Knott JA, Wysocki KM, O'Toole E, Porter ME. 1999. Domains in the 1α dynein heavy chain required for inner arm assembly and flagellar motility in *Chlamydomonas*. J Cell Biol 146:801–818.

Ogawa K. 1991. Four ATP-binding sites in the midregion of the β heavy chain of dynein. Nature 352:643–645.

Omoto CK, Yagi T, Kurimoto E, Kamiya R. 1996. Ability of paralyzed flagella mutants of *Chlamydomonas* to move. Cell Motil Cytoskeleton 33:88–94.

Piperno G, Mead K, Shestak W. 1992. The inner dynein arms I2 interact with a "dynein regulatory complex" in *Chlamydomonas* flagella. J Cell Biol 118:1455–1463.

Ray S, Meyhöfer E, Milligan RA, Howard J. 1993. Kinesin follows the microtubule's protofilament axis. J Cell Biol 121:1083–1093.

Read SM, Northcote DH. 1981. Minimization of variation in the response to different proteins of the Coomassie blue G dye-binding assay for protein. Anal Biochem 116:53–64.

Sakakibara H, Kojima H, Sakai Y, Katayama E, Oiwa K. 1999. Inner-arm dynein c of *Chlamydomonas* flagella is a single-headed processive motor. Nature 400:586–590.

Samsó M, Radermacher M, Frank J, Koonce MP. 1998. Structural characterization of a dynein motor domain. J Mol Biol 276: 927–937.

Sheetz MP, Block SM, Spudich JA. 1986. Myosin movement in vitro: A quantitative assay using oriented actin cables from *Nitella*. Methods Enzymol 134:531–544.

Shingyoji C, Higuchi H, Yoshimura M, Katayama E, Yanagida T. 1998. Dynein arms are oscillating force generators. Nature 393:711–714.

Sloboda RD, Rosenbaum JL. 1982. Purification and assay of microtubule-associated proteins (MAPs). Methods Enzymol 85:409–416.

Toyoshima YY. 1987. Chymotryptic digestion of *Tetrahymena* 22S dynein. I. Decomposition of three-headed 22S dynein to one- and two-headed particles. J Cell Biol 105:887–895.

Vale RD, Toyoshima YY. 1988. Rotation and translocation of microtubules in vitro induced by dyneins from *Tetrahymena* cilia. Cell 52:459–469.

Walker RA, Salmon ED, Endow SA. 1990. The *Drosophila claret* segregation protein is a minus-end directed motor molecule. Nature 347:780–782.

Xu W, Royalty MP, Zimmerman JR, Angus SP, Pennock DG. 1999. The dynein heavy chain gene family in *Tetrahymena thermophila*. J Eukaryot Microbiol 46:606–611.

Yagi T. 2000. ADP-dependent microtubule translocation by flagellar inner-arm dyneins. Cell Struct Funct 25:263–267.